PANM 22

Karel Vacek; Petr Sváček

On fluid structure interaction problems of the heated cylinder approximated by the finite element method

In: Jan Chleboun and Jan Papež and Karel Segeth and Jakub Šístek and Tomáš Vejchodský (eds.): Programs and Algorithms of Numerical Mathematics, Proceedings of Seminar. Hejnice, June 23-28, 2024. , Prague, 2025. pp. 159–168.

Persistent URL: http://dml.cz/dmlcz/703218

Programs and Algorithms of Numerical Mathematics 22
J. Chleboun, J. Papež, K. Segeth, J. Šístek, T. Vejchodský (Eds.)
Institute of Mathematics CAS, Prague 2025

ON FLUID STRUCTURE INTERACTION PROBLEMS OF THE HEATED CYLINDER APPROXIMATED BY THE FINITE ELEMENT METHOD

Karel Vacek[1], Petr Sváček[2]

[1] Institute of Mathematics of the Czech Academy of Sciences, Žitná 25, Prague 1
[2] Czech Technical University
Department of Technical Mathematics, Karlovo náměstí 13, 121 35 Praha 2
karel.vacek@fs.cvut.cz, petr.svacek@fs.cvut.cz

Abstract: This study addresses the problem of the flow around circular cylinders with mixed convection. The focus is on suppressing the vortex-induced vibration (VIV) of the cylinder through heating. The problem is mathematically described using the arbitrary Lagrangian-Eulerian (ALE) method and Boussinesq approximation for simulating fluid flow and heat transfer. The fluid flow is modeled via incompressible Navier-Stokes equations in the ALE formulation with source term, which represent the density variation due to the change of temperature. The temperature is driven by the additional governing transport equation. The equations are numerically discretized by the finite element (FEM) method, where for the velocity-pressure couple the Taylor-Hood (TH) finite element is used and the temperature is approximated by the quadratic elements. The proposed solver is tested on benchmark problems.

Keywords: finite element method, Taylor-Hood element, arbitrary Lagrangian-Eulerian method, heated cylinder

MSC: 65N15, 65M15, 65F08

1. Introduction

The problem of flow around circular cylinders with mixed convection is of considerable importance in various engineering applications, such as flow in tubes, heat exchangers, nuclear reactor fuel rods, chimney stacks, cooling towers, etc. These applications involve critical engineering design parameters related to fluid flow, heat transfer, and vibration, which must be carefully considered, see [4].

This paper focuses on the suppression of vortex-induced vibration (VIV) of the cylinder by its heating. Over the years, numerous numerical and experimental studies have focused on investigating homogeneous or uniform flow around a circular cylinder that is movable in a vertical direction (see, e.g., [1,3]). In these studies, flow

DOI: 10.21136/panm.2024.15

behavior is primarily characterized by the Reynolds number (Re), and structure motion is always non-dimensional, where its stiffness is characterized by the reduced velocity U_r. The response of the system and its resonance is dependent only on these two variables, see [1]. However, if one considers the buoyancy forces, there is another non-dimensional parameter, called the Grashof number (Gr), which can be used for controlling the fluid flow and the structural response. For example, in [10] it is shown that for $Re = 100$ and for the $Gr \geq 1500$ the vortex shedding is stopped and the flow becomes steady state. An increase in the Gr number also leads to an increase in the drag coefficient. Similar results were found in [11] where for $Re = 200$ the critical value $Gr = 12000$ was determined. The results of the heated movable cylinder can be found, e.g., in [14], where the critical Gr number was defined to be dependent also on the reduced velocity.

This paper focuses on a numerical simulation of the VIV problems of the cylinder leading to suppression of the vibrations, a description of such strategies can be found in [4]. A simplified model of incompressible fluid with buoyancy forces is considered, however, for such a model still several numerical challenges, such as managing the incompressibility constraint, nonlinear convective terms and coupling between the additional transport equation of the temperature with the momentum equations need to be addressed (see, e.g., [10]). The model needs to treat the time-dependent computational fluid domain, which is usually handled using the arbitrary Lagrangian-Eulerian (ALE) method, see e.g., [13]. To describe the fluid flow influenced by the heat transfer, the Boussinesq approximation is used. The mathematical model consists of the incompressible Navier-Stokes equations with a right-hand side term depending on the temperature. The temperature is described by an additional transport equation. For the approximation of the system of incompressible Navier-Stokes equations in the ALE formulation, the Taylor-Hood (TH) finite element is used. This choice of the velocity-pressure pair satisfies the Babuška-Brezzi (BB) inf-sup condition, which guarantees the stability of the numerical scheme, see [8]. The temperature is approximated by continuous piecewise quadratic functions.

The proposed method is tested on two benchmark problems. The first involves the flow around a fixed heated cylinder, where the critical Grashof number and mean drag coefficient are compared with the data from [10]. In the second test case, the suppression of vibration of a moving cylinder is addressed by its heating, the response is compared with the findings of [14].

2. Governing equations

In this section, the mathematical model of the fluid flow around the heated moving cylinder is given, where the density changes due to the temperature described by the Boussinesq approximation. The model consists of the incompressible Navier-Stokes equations in the ALE formulation coupled with the convection-diffusion equation for the temperature.

Let $\Omega_t \subset \mathbb{R}^2$ be a bounded computational time-dependent fluid domain with a continuous Lipschitz boundary, which is composed of three disjoint segments: $\partial\Omega = \Gamma_D \cup \Gamma_O \cup \Gamma_{W_t}$. The domain Ω_t is assumed to be polygonal, and completely filled with fluid at any time $t \in (0, T_\infty)$. The movability of the domain is treated via the Arbitrary Lagrangian-Eulerian (ALE) formulation. The ALE method uses a mapping A_t that transforms the reference domain Ω_0 on the current domain Ω_t, i.e.,

$$A_t \colon \Omega_{\mathrm{ref}} \to \Omega_t, \quad X \mapsto x(X,t) = A_t(X), \quad x \in \Omega_{\mathrm{ref}},\ t \in (0, T_\infty]),$$

moreover transforms the reference interface Γ_{W_0} on the current interface Γ_{W_t} based on the movement of the cylinder, while the other boundaries remain stationary. For further details, see [13].

For computation, the non-dimensional Navier-Stokes (NS) equations for incompressible flow and the thermal equation in the ALE formulation are used. Firstly, all lengths are characterized by the cylinder diameter D, the flow velocities $\boldsymbol{u} = (u_1, u_2)$ are scaled by the free stream velocity U_{ref}, the time is scaled by the factor D/U_{ref}, and the kinematic pressure is scaled by ρU_{ref}^2, where ρ is the fluid density. In addition, the non-dimensional temperature is given by $\theta = (T - T_{\mathrm{ref}})/(T_s - T_{\mathrm{ref}})$, where T represents fluid temperature, T_{ref} is the temperature of the free stream, and T_s is the temperature of the cylinder. For simplicity, in the rest of the paper, all of the quantities are dimensionless. The nondimensional form of the NS equations with the transport temperature equation read: Find the velocity $\boldsymbol{u}(x,t) \colon \Omega_t \to \mathbb{R}^2$, the pressure $p(x,t) \colon \Omega_t \to \mathbb{R}$, and the temperature $\theta(x,t) \colon \Omega_t \to \mathbb{R}$ which satisfy

$$\begin{aligned}
\frac{D^A}{Dt}\boldsymbol{u} + [(\boldsymbol{u} - \boldsymbol{w}) \cdot \boldsymbol{\nabla}]\boldsymbol{u} - \frac{1}{Re}\boldsymbol{\Delta u} + \boldsymbol{\nabla} p &= \frac{Gr}{Re^2}\theta && \text{in } \Omega_t, t \in (0, T_\infty], \\
\boldsymbol{\nabla} \cdot \boldsymbol{u} &= 0 && \text{in } \Omega_t, t \in (0, T_\infty], \\
\frac{D^A}{Dt}\theta + [(\boldsymbol{u} - \boldsymbol{w}) \cdot \boldsymbol{\nabla}]\theta - \frac{1}{RePr}\boldsymbol{\Delta}\theta &= 0 && \text{in } \Omega_t, t \in (0, T_\infty],
\end{aligned} \tag{1}$$

where $\frac{D^A}{Dt}$ denotes the ALE derivative, and $\boldsymbol{w} = \partial A^t/\partial t$ represents the domain velocity, see [2,13]. The Re, Pr, and Gr are the Reynolds, Prandtl and Grashof numbers respectively, given as $Re = U_{\mathrm{ref}}D/\nu$, $\mathrm{Pr} = \nu/\kappa$, and $Gr = g\beta\Delta T D^3/\nu^2$, where ν is the kinematic viscosity, κ is the thermal diffusivity, ΔT is the temperature difference ($\Delta T = T_s - T_{\mathrm{ref}}$), β means the thermal expansion coefficient and g is the gravitational acceleration (in this paper acting in the horizontal direction), see [14]. This approximation of the flow problem around the heated cylinder is valid for approximately $\beta\Delta T \leq 0.01$, see [10].

To close problem (1), the following conditions are added: initial condition

$$\boldsymbol{u}(x,0) = \boldsymbol{u}_0, \quad \theta(x,0) = \theta_0 \quad \text{in } \Omega_0, \tag{2}$$

and the boundary conditions

$$\boldsymbol{u}(x,t) = \boldsymbol{g}(x,t), \quad \theta(x,t) = q(x,t) \quad \text{on } \Gamma_D \times (0,T_\infty], \tag{3a}$$

$$\boldsymbol{u}(x,t) = \boldsymbol{w}(x,t), \quad \theta(x,t) = q(x,t) \quad \text{on } \Gamma_{W_t},\ t \in (0,T_\infty], \tag{3b}$$

$$\frac{\partial \theta}{\partial n} = 0 \quad \text{on } \Gamma_O \times (0,T_\infty], \tag{3c}$$

$$-(p - p_{\text{ref}})\boldsymbol{n} + \frac{1}{Re}\frac{\partial \boldsymbol{u}}{\partial \boldsymbol{n}} = 0 \quad \text{on } \Gamma_O \times (0,T_\infty], \tag{3d}$$

where $\boldsymbol{n}$ represents the unit outward normal vector to $\partial\Omega_t$ and p_{ref} represents a reference pressure value at the outlet. Here, Eq. (3a) is the no-slip condition, (3b) reflects the assumption that the fluid remains attached to the cylinder, (3c) is the Neumann condition, and (3d) is the so-called do-nothing condition, see [6].

2.1. Motion of the cylinder

In this paper, a simplified model can be used as the cylinder is movable only in the vertical direction. Therefore, the ordinary differential equation (ODE) for the displacement Y, its velocity $\dot{Y}$ and acceleration $\ddot{Y}$ in non-dimensional form are

$$\ddot{Y} + \left(\frac{4\pi\xi}{U_r}\right)\dot{Y} + \left(\frac{4\pi^2}{U_r^2}\right)Y = \frac{C_l}{2M^*}, \tag{4}$$

where ξ symbolizes the structural damping ratio, $U_r = \frac{U_\infty}{f_n D}$ is the reduced velocity of the cylinder (with f_n representing the natural frequency of the cylinder), M^* indicates for the reduced mass of the rigid cylinder ($M^* = \frac{m}{\rho D^2}$), and $C_l = \frac{L}{1/2\rho U_\infty^2 A}$ is the lift coefficient (here L represents the lift force), see [1,14].

3. Discretization of the fluid flow problem

In order to discretize problem (1) by the finite element method (FEM), the weak formulation has to be introduced. First, a constant time step $\Delta t > 0$ is taken, and the time interval $(0,T_\infty)$ is equidistantly divided into time intervals (t_n, t_{n+1}) with $t_n = n\Delta t$. Further, the velocity, pressure and the temperature are approximated at time step $t_n \in (0,T_\infty]$ by $\boldsymbol{u}^n(x) \approx \boldsymbol{u}(x,t_n)$ for $x \in \Omega_{t_n}$, $p^n(x) \approx p(x,t_n)$ for $x \in \Omega_{t_n}$, and $\theta^n(x) \approx \theta(x,t_n)$ for $x \in \Omega_{t_n}$. The velocity of the domain at the instant t_{n+1} is approximated by $\boldsymbol{w}^{n+1}(x) \approx \boldsymbol{w}(x,t_{n+1})$ for $x \in \Omega_{t_{n+1}}$ and the ALE derivative is approximated at fixed time instance t_{n+1} by the second-order two-step backward difference formula (BDF2). Hence, the implicit scheme is given

$$\begin{aligned}
\frac{3\boldsymbol{u}^{n+1} - 4\tilde{\boldsymbol{u}}^n + \tilde{\boldsymbol{u}}^{n-1}}{2\Delta t} + ((\boldsymbol{u}^{n+1} - \boldsymbol{w}^{n+1})\cdot\boldsymbol{\nabla})\boldsymbol{u}^{n+1} - \frac{1}{\text{Re}}\boldsymbol{\Delta}\boldsymbol{u}^{n+1} + \boldsymbol{\nabla}p^{n+1} &= \frac{Gr}{Re^2}\theta, \\
\boldsymbol{\nabla}\cdot\boldsymbol{u}^{n+1} &= 0, \\
\frac{3\theta^{n+1} - 4\tilde{\theta}^n + \tilde{\theta}^{n-1}}{2\Delta t} + ((\boldsymbol{u}^{n+1} - \boldsymbol{w}^{n+1})\cdot\boldsymbol{\nabla})\theta^{n+1} - \frac{1}{\text{RePr}}\boldsymbol{\Delta}\theta^{n+1} &= 0,
\end{aligned}$$

where $\tilde{\boldsymbol{u}}^i$ and $\tilde{\theta}^i$ denotes the transformation of u^i and θ^i from Ω_i onto Ω_{n+1}, i.e., $\tilde{\boldsymbol{u}}^i = \boldsymbol{u}^i \circ A_{t_i} \circ A_{t_{n+1}}^{-1}$.

3.1. Spatial discretization by the FEM

In this section, the FEM discretization of the semi-discrete problem (5) is introduced in the standard way. Firstly, a weak formulation is provided. Let us assume the fixed time instance t_{n+1}, and present a simplified notation: $\boldsymbol{u} = \boldsymbol{u}^{n+1}$, $\boldsymbol{w} = \boldsymbol{w}^{n+1}$, $p = p^{n+1}$, and $\Omega = \Omega_{t_{n+1}}$.

Furthermore, the velocity test space $\boldsymbol{\mathcal{V}}$, the pressure test space $\mathcal{Q}$ and the temperature test space $\mathscr{T}$ are defined as

$$
\begin{aligned}
\boldsymbol{\mathcal{V}} &= \left\{\boldsymbol{\varphi} \in \boldsymbol{H}^1(\Omega)\ \boldsymbol{\varphi}(x) = 0\ \forall x \in \Gamma_D \cup \Gamma_W\right\}, \quad \mathcal{Q} = L^2(\Omega),\\
\mathscr{T} &= \left\{\varphi \in H^1(\Omega)\ \varphi(x) = 0\ \forall x \in \Gamma_D \cup \Gamma_W\right\},
\end{aligned}
$$

where $\boldsymbol{H}^1(\Omega) = [H^1(\Omega)]^2$ is the vector Sobolev space and $L^2(\Omega)$ is the Lebesgue space, see [9].

Using some mathematical operation and proposing the notation of the scalar product $(\boldsymbol{u}, \boldsymbol{v})_\Omega = \int_\Omega \boldsymbol{u} \cdot \boldsymbol{v}\, \mathrm{d}x$ in $L^2(\Omega)$ and of the trilinear form $c(\boldsymbol{u}, \boldsymbol{v}, \boldsymbol{w}) = \int_\Omega [(\boldsymbol{u} \cdot \nabla)\boldsymbol{v}] \cdot \boldsymbol{w}\ \mathrm{d}x$, the weak formulation reads: Find $U = (\boldsymbol{u}, p.\theta) \in \boldsymbol{\mathcal{V}} \times \mathscr{Q} \times \mathscr{T}$ such that the equation

$$
a\left(\boldsymbol{u}, U, V\right) + a_\theta\left(\boldsymbol{u}, U, V\right) = F(V) + F_\theta(V), \tag{5}
$$

holds for any test function $V = (\boldsymbol{v}, q, \zeta) \in \boldsymbol{\mathcal{V}} \times \mathscr{Q} \times \mathscr{T}$, where

$$
\begin{aligned}
a\left(U, V\right) &= \frac{3}{2\Delta t}(\boldsymbol{u}, \boldsymbol{v})_\Omega + \frac{1}{\mathrm{Re}}(\nabla \boldsymbol{u}, \nabla \boldsymbol{v})_\Omega + c(\boldsymbol{u} - \boldsymbol{w}, \boldsymbol{u}, \boldsymbol{v}) - (p, \nabla \cdot \boldsymbol{v})_\Omega - (\nabla \cdot \boldsymbol{u}, q)_\Omega,\\
F\left(V\right) &= \frac{1}{2\Delta t}(4\tilde{\boldsymbol{u}}^n - \tilde{\boldsymbol{u}}^{n-1}, \boldsymbol{v})_\Omega + \frac{Gr}{Re^2}(\theta, \boldsymbol{v})_\Omega,
\end{aligned} \tag{6}
$$

and

$$
\begin{aligned}
a_\theta\left(\boldsymbol{u}, \theta, \zeta\right) &= \frac{3}{2\Delta t}(\theta, \zeta)_\Omega + \frac{1}{RePr}(\nabla\theta, \nabla\zeta)_\Omega + ((\boldsymbol{u} \cdot \nabla)\theta, \zeta)_\Omega,\\
F_\theta(\zeta) &= \frac{1}{2\Delta t}(4\tilde{\theta}^n - \tilde{\theta}^{n-1}, \zeta)_\Omega.
\end{aligned} \tag{7}
$$

For a more detailed description see [8].

In addition, the admissible triangulation τ_h of the domain Ω is considered (see [5]) and in this triangulation, the following finite element (FE) subspaces are used: $\boldsymbol{\mathcal{V}}_h \subset \boldsymbol{\mathcal{V}}$ as the velocity subspace, $\mathcal{Q}_h \subset \mathcal{Q}$ as the pressure subspace, and $\mathscr{T}_h \subset \mathscr{T}$ as the temperature subspace. Generally, finite element subspaces consist of piecewise polynomial functions. In this paper, the velocity and the pressure are discretized by the so-called Taylor-Hood element which leads to the following function spaces

$$
\boldsymbol{\mathcal{V}}_h = \left\{\boldsymbol{\varphi} \in \mathbf{C}(\overline{\Omega})\ (\boldsymbol{\varphi}\big|_K \in P_2(K), \forall K \in \tau_h)\right\} \cap \boldsymbol{\mathcal{V}}, \tag{8}
$$

$$
\mathcal{Q}_h = \left\{\varphi \in C(\overline{\Omega})\ (\varphi\big|_K \in P_1(K), \forall K \in \tau_h)\right\}. \tag{9}
$$

The temperature is discretized by the piecewise quadratic functions

$$\mathscr{T}_h = \left\{ \varphi \in \mathbf{C}(\overline{\Omega}) \left(\varphi\big|_K \in P_2(K), \forall K \in \tau_h \right) \right\} \cap \mathscr{T}. \tag{10}$$

Then, the discrete problem reads: Find $U_h = (\boldsymbol{u}_h, p_h, \theta_h) \in \boldsymbol{\mathcal{V}}_h \times \mathscr{Q}_h \times \mathscr{T}_h$ such that the equations

$$a_h\left(U_h, V_h\right) + a_\theta\left(\boldsymbol{u}_h, \theta_h, \zeta_h\right) = F(V_h, \theta_h) + F_{\theta_h}(\zeta_h) \tag{11}$$

hold for any test function $V_h = (\boldsymbol{v}_h, q_h, \zeta_h) \in \boldsymbol{\mathcal{V}}_h \times \mathscr{Q}_h \times \mathscr{T}_h$ and satisfies the boundary conditions (3a)–(3c).

4. Numerical simulations

In this section, the results of numerical simulations are discussed, such as the problem of flow around the fixed heated cylinder and flow around the heated cylinder with one degree of freedom in the cross direction. The domain of the problem is shown in Figure 1. The fluid flow around the heated cylinder is modeled using Eqs. (1), which are incompressible Navier-Stokes equations, incorporating the Boussinesq approximation to account for temperature variations. For the fixed case the Γ_{W_t} remains stationary while in the problem with vibrations, it can move in the vertical direction.

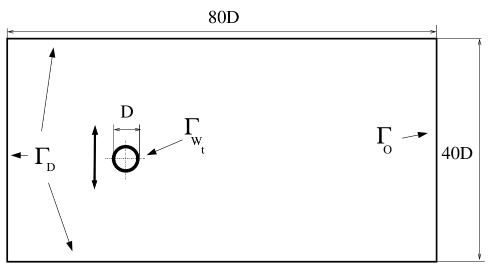

Figure 1: Domain of the flow around the cylinder.

4.1. Flow around the heated cylinder

The first test case is the flow around the fixed cylinder. The boundary conditions include the Dirichlet boundary conditions on Γ_D. The Γ_{W_t} incorporates the movable surface (for a simple case without moving, the surface is fixed). At the outlet Γ_O, the so-called do-nothing condition is used for the velocity and pressure (see [12]). The temperature is subject to Dirichlet boundary conditions in the free stream $\Gamma_{D,1}$ and at the Γ_{W_t}, while a Neumann boundary condition is applied at the outlet Γ_O. The domain size was selected based on [11], and the size of the mesh was limited by the solver, which the UMFPACK library provides, and it performs efficiently up to 200000 DoFs.

Calculations were performed for various scenarios involving different Grashof numbers, with Reynolds numbers $Re = 100$ and $Re = 200$. The critical Gr number

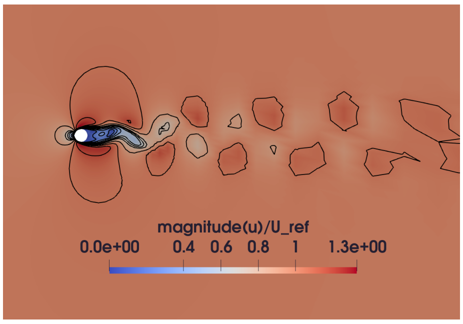

Figure 2: Magnitude of the velocity ($||\boldsymbol{u}||_\infty$) for the $Gr = 1000$.

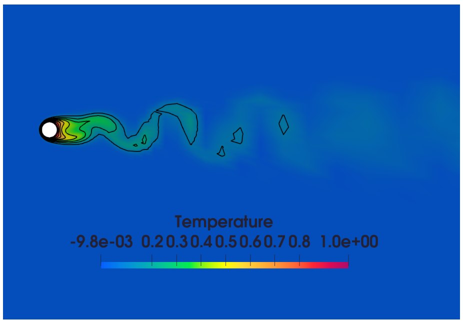

Figure 3: Temperature field θ for the $Gr = 1000$.

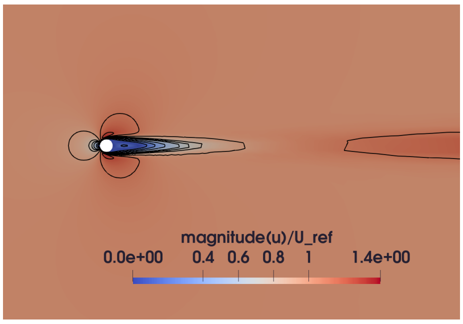

Figure 4: Magnitude of the velocity ($||\boldsymbol{u}||_\infty$) for the $Gr = 1500$.

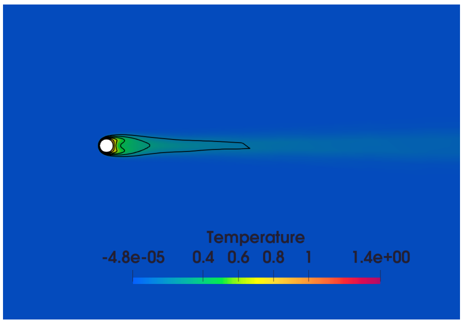

Figure 5: Temperature field θ for the $Gr = 1500$.

(the lowest number where the flow becomes steady) is compared with [10] and the drag coefficients for various scenarios are also compared. Figures 2–5 show the results for four cases with $Re = 100$. As the Grashof number increases, the flow gradually stabilizes until it reaches a critical Grashof number ($Gr = 1500$), after which the flow is nearly steady. This corresponds to [10]. Similar trends were observed for $Re = 200$, although the critical Grashof number is higher ($Gr = 15000$), probably due to the insufficient quality of the mesh. Despite this, the mean drag coefficient for both cases is aligned well with the reference data [10, 11], see Figure 6.

4.2. Flow around the movable heated cylinder

The initial state of the domain, denoted as Ω_t, is in Figure 1 with heated cylinder. The boundary conditions are similar to the previous problem, and due to the movement of the cylinder, the Dirichlet boundary condition is $\boldsymbol{u} = \boldsymbol{w}$. Its position is obtained by solving the problem (4) using the 4-th order Runge-Kutta method. The coupling procedure between the cylinder and the fluid flow is performed using a strong coupling algorithm, which is well described in [7]. The mesh movement is realized by the pseudo-elastic approach, which is described, e.g., in [7].

The flow problem around the cylinder is characterized by the Reynolds number $\mathrm{Re} = 150$, aligned with the reference data from [14]. The model of a movable cylinder

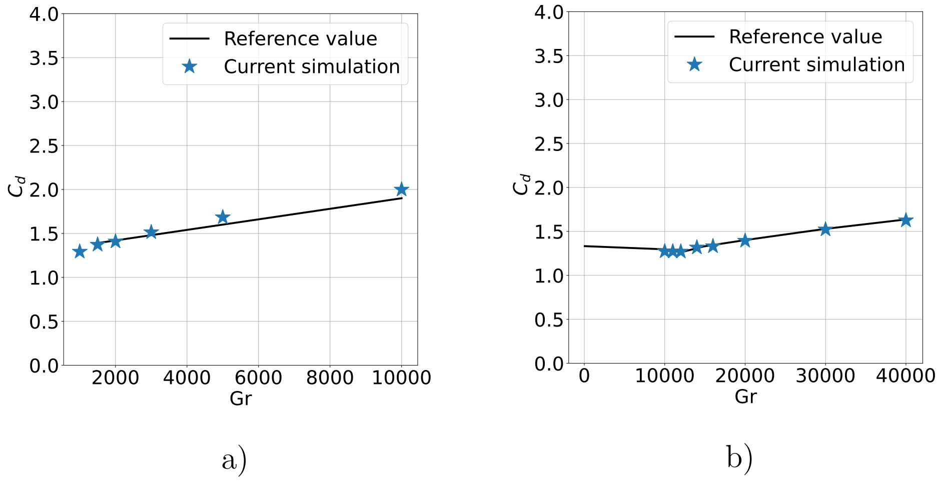

Figure 6: Drag coefficient for different Gr numbers for $Re = 100$ a), and for $Re = 200$ b), compared to the reference data from [10, 11].

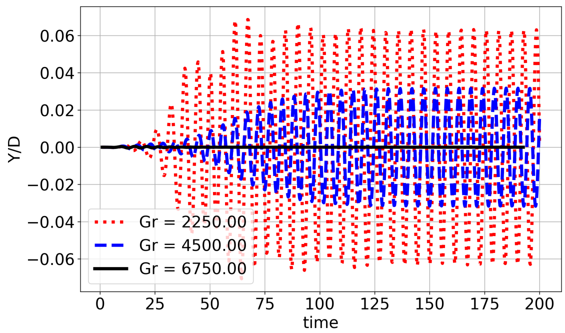

Figure 7: Displacement Y/D in dependent of time for the case $U_r = 8$ and $Re = 150$.

without heating is well described in [1]. A vortex street forms in the wake of the cylinder, leading to oscillations in aerodynamic forces, which in turn induce the vibration of the cylinder. The interval in which the resonance occurs is $U_r \in [4, 8]$. The highest amplitude is for $U_r = 4$ and then the amplitude decreases with increasing U_r, see [1].

Our goal is to suppress the vibration by heating and stabilizing the flow. In Figure 7, the displacement Y is given for $U_r = 8$, with zero damping $\xi = 0$, and $M^* = 2$.

It can be observed, that as the Gr is increased (we add more and more heating), the vortex shedding is stabilized until we reach the $Gr = 6750$ and we reach an almost steady state. This result corresponds to [14].

5. Conclusion

In this paper, the problem of the interaction between incompressible flow and a heated cylinder with one degree of freedom is analyzed using numerical simulations. The main goal was to suppress the flow-induced vibrations (VIV) by its heating.

The problem was mathematically described as the incompressible fluid which is approximated by the incompressible Navier-Stokes (NS) equations, where to take into account the density dependence on the temperature, the Boussinesq approximation was used. As a result, a source term depending on the temperature is included in the NS equations, where the temperature is modeled by an additional transport equation. For time discretization the backward-difference formula of second order (BDF2) is used, whereas for space discretization the finite element method (FEM) is utilized. The velocity and pressure are discretized by the Taylor-Hood (TH) element, while the temperature is discretized by the piecewise quadratic functions. The numerical results of the developed in-house solver are presented and compared with the reference data of [10, 14].

For the first case of the flow around the fixed cylinder, it was confirmed that the stability of the flow is dependent in addition to the Reynolds number (Re) also on the Grashof number (Gr). It was observed that for $Re = 100$ the critical Gr number is $Gr = 1500$, which is in agreement with [10]. For the case, $Re = 200$, the obtained critical Gr number ($Gr = 15000$) is larger than the value $Gr = 12000$ found in [11]. This is probably due to the use of a not sufficiently refined mesh, where the applied solver is limited by the number of unknowns from the UMFPACK library. In addition, the dependence of the drag coefficient on the Grashof number was compared with the reference data from [10, 11]. It was shown that with an increase in the Gr number, the drag coefficient also increases. Our simulations slightly overestimated the drag for $Re = 200$, it might again be attributed to insufficient quality of the mesh.

The second case was the flow around a vibrating cylinder, whose vibrations are described using one degree of freedom (vertical displacement). The structural movement is characterized by the reduced velocity U_r. It is shown that for one case of reduced velocity (i.e., $U_r = 8$) the amplitude of the response is lowered with an increase of the Gr number. Such a decrease of vibrations continues with further increase up to the critical Gr number $Gr = 6750$, for which an almost steady state is obtained. This is also in agreement with the findings in [14].

It was shown that the presented results of the developed in-house numerical solver agree with the reference data. Further, the numerical results showed that the heating of the cylinder can lead to the suppression of the VIV of the cylinder. The main limitation of the presented solver is that it can solve only small systems due to the UMFPACK library used as a solver. This problem can be addressed, e.g., by domain decomposition.

Acknowledgements

The authors acknowledge the support by the Grant Agency of the Czech Technical University in Prague, grant No. SGS SGS22/148/OHK2/3T/12, and grant No. SGS SGS24/120/OHK2/3T/12. Karel Vacek has also been supported by the Czech Science Foundation (GAČR) project 22-01591S. The Institute of Mathematics of the CAS is supported by RVO:67985840.

References

[1] Ahn, H. T. and Kallinderis, Y.: Strongly coupled flow-structure interactions with a geometrically conservative ALE scheme on general hybrid meshes. J. Comput. Phys. **219** (2006), 671–696.

[2] Alsabery, A., Sheremet, M., Ghalambaz, M., Chamkha, A., and Hashim, I.: Fluid-structure interaction in natural convection heat transfer in an oblique cavity with a flexible oscillating fin and partial heating. Applied Thermal Engineering **145** (2018), 80–97.

[3] Bao, Y., Huang, C., Zhou, D., Tu, J., and Han, Z.: Two-degree-of-freedom flow-induced vibrations on isolated and tandem cylinders with varying natural frequency ratios. J. Fluids Struct. **35** (2012), 50–75.

[4] Chen, W. L., Huang, Y., Chen, C., Yu, H., and Gao, D.: Review of active control of circular cylinder flow. Ocean Engineering **258** (2022), 111 840.

[5] Ciarlet, P. G.: *The finite element method for elliptic problems*. Society for Industrial and Applied Mathematics, 2002.

[6] Feistauer, M.: *Mathematical methods in fluid dynamics*. 67, Chapman and Hall/CRC, 1993.

[7] Feistauer, M., Horáček, J., Růžička, M., and Sváček, P.: Numerical analysis of flow-induced nonlinear vibrations of an airfoil with three degrees of freedom. Comput. Fluids **49** (2011), 110–127.

[8] Girault, V. and Raviart, P.: *Finite Element Methods for Navier-Stokes Equations: Theory and Algorithms*. Computational Mathematics Series, Springer-Verlag, 1986.

[9] Kufner, A., John, O., and Fucik, S.: *Function spaces*. Mechanics: Analysis, Springer Netherlands, 1977.

[10] Patnaik, B. V., Narayana, P. A., and Seetharamu, K.: Numerical simulation of vortex shedding past a circular cylinder under the influence of buoyancy. Int. J. Heat Mass Transfer **42** (1999), 3495–3507.

[11] Salimipour, E.: A numerical study on the fluid flow and heat transfer from a horizontal circular cylinder under mixed convection. Int. J. Heat and Mass Transfer **131** (2019), 365–374.

[12] Sváček, P., Feistauer, M., and Horáček, J.: Numerical simulation of flow induced airfoil vibrations with large amplitudes. J. Fluids Struct. **23** (2007), 391–411.

[13] Takashi, N. and Hughes, T. J.: An arbitrary Lagrangian-Eulerian finite element method for interaction of fluid and a rigid body. Comput. Methods in Appl. Mech. Eng. **95** (1992), 115–138.

[14] Wan, H. and Patnaik, S. S.: Suppression of vortex-induced vibration of a circular cylinder using thermal effects. Phys. Fluids **28** (2016).